Crack Deflection at an Interface Between Two Orthotropic Media

V. Gupta[1]
Assoc. Mem. ASME.

A. S. Argon
Massachusetts Institute of Technology, Cambridge, MA 02139

Z. Suo[2]
Harvard University, Cambridge, MA 02138

To achieve toughness in many brittle composites, crack deflection at interfaces is essential. For this, it is necessary to establish crack deflection criteria by employing the principles of interfacial fracture mechanics applicable to anisotropic pair of materials. Such an analysis, with two aligned orthotropic media, is considered here. The stress and deformation fields derived for such cases are shown to depend on material parameters λ and ρ for the two media and on the two so-called Dundur constants α and β. For $\beta = 0$, the dependence on λ_1 and λ_2 collapses to $\Lambda = (\lambda_1/\lambda_2)^{1/4}$. The delamination criterion is insensitive to λ, ρ, Λ, and β over practical ranges of these material parameters. Thus, generalized delamination charts become possible as a function of the bi-material constant α alone, which characterizes the elastic dissimilarity between the two media. Using these charts, it is possible to determine the desired level of the interface strength required in composite manufacturing in order to enhance the overall toughness of a composite. Furthermore, such charts can be used for the interfaces between fiber/coating, fiber/matrix, or matrix/coating, depending on which interface is of critical interest for the crack deflection. It is shown how these charts can be used to identify composite systems where it is possible to maximize both the transverse strength and the longitudinal toughness.

1 Introduction

It is now widely appreciated that the mechanical properties of interfaces play a key role in the overall performance of a composite material, and that the desirable levels of toughness in composites can be obtained through the tailoring of interface properties. Interfaces across which the physical and mechanical properties of component phases change abruptly can be either the sites of unwanted premature separation due to deformation-induced stress concentration or they can be made to act in a beneficial sense to arrest or deflect cracks. The various strategies on how damaged parts of a composite can be controllably decoupled from undamaged parts by promoting delamination across interfaces, have been discussed by many investigators (see, e.g., Cook and Gordon, 1964; Gupta et al., 1989). The two basic choices for a crack are shown in Fig. 1, where a brittle crack momentarily impinges on an interface between a matrix or a coating and a reinforcing fiber at right angles. The crack can either propagate ahead into the fiber or be deflected along the interface and continue to propagate along it in a benign manner. Strategies to achieve the second and desirable alternative rely on two complementary criteria based on either local crack-tip stresses or differences of work of fracture along possible alternative crack paths.

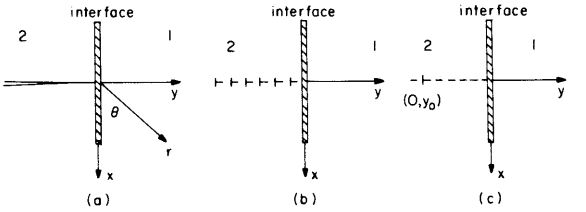

Fig. 1(*a*) Semi-infinite crack terminating perpendicular to the interface between two orthotropic materials with aligned principal axis, (*b*) semi-infinite crack represented as a continuous distribution of edge dislocations, and (*c*) a single edge dislocation in the vicinity of an interface

The local stress criterion for crack deflection demands that, under the probing of the crack-tip stress field, the decohesion stress for tensile or for shear separation along the interface be reached before the cohesive strength is reached in the fiber at the crack tip. The complementary fracture work criterion, on the other hand, demands that, when the crack is about to grow, for virtual extensions of a crack ahead in its plane or along the interface, the work of fracture should be less along the interface than ahead into the fiber. Here we will pursue only the local stress criterion, particularly in the context of highly anisotropic fibers (e.g., for the Pitch-55 carbon fiber which has an axial modulus of 380 GPa and a transverse modulus of only 20 GPa). The degree of anisotropy considered here is restricted to the orthotropic level, as most cases of current interest fall in this category.

[1]Presently at the Thayer School of Engineering, Dartmouth College, Hanover, NH 03755.

[2]Presently at the Department of Mechanical and Environmental Engineering, University of California at Santa Barbara, Santa Barbara, CA 93106.

Contributed by the Applied Mechanics Division of THE AMERICAN SOCIETY OF MECHANICAL ENGINEERS for presentation at the Winter Annual Meeting, Atlanta, Ga., Dec. 1-6, 1991.

Discussion on this paper should be addressed to the Technical Editor, Prof. Leon M. Keer, The Technological Institute, Northwestern University, Evanston, IL 60208, and will be accepted until two months after final publication of the paper itself in the JOURNAL OF APPLIED MECHANICS. Manuscript received by the ASME Applied Mechanics Division, Oct. 16, 1990; final revision, May 24, 1991.

Paper No. 91-WA/APM-42.

The problem of a crack terminating at right angles on an interface between two dissimilar, but isotropic media, has been solved in the past by several investigators (Zak and Williams, 1963; Swenson and Rau, 1970; Erdogan and Biricikoglu, 1973). Solutions to the corresponding problem for a pair of anisotropic materials also exist (Ting and Hoang, 1984; Erdogan, 1972). While they are equally useful for the statement of the crack deflection criterion by interface delamination, they are less adequate to the solution of the problem of the energy release upon crack extension than the approach using continuously distributed dislocations that we will develop here. In this communication, however, we will not pursue the question of energy release. Here we present new results for the problem of a crack impinging at normal incidence on an interface between two orthotropic media with principal material axes parallel and perpendicular to the interface for the purpose of developing the crack deflection criterion applicable to specific cases such as the pair of SiC coating and pitch-55 fiber.

Furthermore, we identify critical anisotropic elastic constants influencing the structure of the solution so as to give generalized results useful for most practical ranges of bi-material combinations of interest to the current composite systems. Clearly, our solutions will be a special case of a more general (but far more difficult) problem of a crack impinging on an interface at an arbitrary angle. Nevertheless, our solution should be widely applicable to aligned fiber composite materials.

2 Crack Normal to a Bi-Material Interface

2.1 Problem Statement and Solution Structure. The basic problem to be analysed is shown in Fig. 1(*a*). A semi-infinite crack terminates normal to the interface between two orthotropic materials with aligned principal axes. Both media are taken to be homogeneous, linear elastic solids. Both plane stress and plane strain deformation are considered. For generally anisotropic materials, Hooke's law can be written as

$$\epsilon_i = \sum_{j=1}^{6} s_{ij}\sigma_j, \quad (i = 1\text{-}6). \tag{1a}$$

Where the standard correspondence is adopted, i.e., $\{\epsilon_i\} = \{\epsilon_x, \epsilon_y, \epsilon_z, \gamma_{yz}, \gamma_{zx}, \gamma_{xy}\}$, $\{\sigma_i\} = \{\sigma_x, \sigma_y, \sigma_z, \tau_{yz}, \tau_{zx}, \tau_{xy}\}$, and s_{ij} are elements of a six-by-six symmetric matrix of compliances with 21 independent elements in the most general case. When the material has orthotropic symmetry, then the elastic stress-strain equations can be reduced to (see Lekhnitskii, 1963)

$$\epsilon_i = \sum_{j=1,2,6} b_{ij}\sigma_j, \quad (i = 1,2,6) \tag{1b}$$

$$b_{ij} = \begin{cases} s_{ij}, \text{ for plane stress} \\ s_{ij} - (s_{i3}s_{j3})/s_{33}, \text{ for plane strain} \end{cases} \quad i,j = 1,2,6 \tag{1c}$$

with only four remaining independent elastic compliances, b_{11}, $b_{12} = b_{21}$, b_{22}, and b_{66} ($b_{16} = b_{26} = 0$); in each of the two media. It was shown by Suo (1988) that for a singly connected domain of an orthotropic medium with prescribed traction on its boundary, the stress in each medium depends on two dimensionless elastic constants λ and ρ, defined as

$$\lambda = s_{11}/s_{22}, \tag{2a}$$

$$\rho = \frac{2s_{12} + s_{66}}{2\sqrt{s_{11}s_{22}}}. \tag{2b}$$

These constants measure the anisotropy in the sense that $\lambda = 1$ when the material has transverse cubic symmetry, and $\lambda = \rho = 1$ when the material becomes transversely isotropic. The positive definiteness of the strain energy density requires that

$$\lambda > 0, \quad -1 < \rho < \infty. \tag{3}$$

Following Lekhnitskii (1963), for plane deformation, the elastic field can be represented in terms of two complex potential functions $\Phi_1(z_1)$, $\Phi_2(z_2)$, each of which is holomorphic in its argument $z_j = x + \mu_j y$. Here, μ_j are two distinct complex numbers with positive imaginary parts, which are obtained as the roots of the following characteristic equation

$$\lambda\mu^4 + 2\rho(\lambda)^{1/2}\mu^2 + 1 = 0. \tag{4}$$

The foregoing equation is a special form of the sixth-order characteristic equation obtained by Lekhnitskii (1963), when the governing differential equation for the stress potential is expressed as six first-order equations. The roots with the positive imaginary parts of Eq. (4) are

$$\mu_1 = i\lambda^{-1/4}(n+m),$$

$$\mu_2 = i\lambda^{-1/4}(n-m), \quad (\text{for } 1 < \rho < \infty) \tag{5a}$$

$$\mu_1 = \lambda^{-1/4}(in+m),$$

$$\mu_2 = \lambda^{-1/4}(in-m), \quad (\text{for } -1 < \rho < 1) \tag{5b}$$

$$\mu_1 = \mu_2 = i\lambda^{-1/4}, \quad (\text{for } \rho = 1) \tag{5c}$$

$$n = \sqrt{\frac{1+\rho}{2}} \quad m = \sqrt{\left|\frac{1-\rho}{2}\right|} \tag{5d}$$

With these holomorphic functions, the representation for the displacements u_i, stresses σ_{ij}, and the resultant forces on an arc f_i (the medium is kept on the left-hand side as an observer travels in the positive direction of the arc) is

$$u_i = 2\ \mathrm{Re}\left[\sum_{j=1}^{2} A_{ij}\Phi_j(z_j)\right] \tag{6a}$$

$$\sigma_{2i} = 2\ \mathrm{Re}\left[\sum_{j=1}^{2} L_{ij}\Phi_j'(z_j)\right] \tag{6b}$$

$$\sigma_{1i} = -2\ \mathrm{Re}\left[\sum_{j=1}^{2} L_{ij}\mu_j\Phi_j'(z_j)\right] \tag{6c}$$

$$f_i = -2\ \mathrm{Re}\left[\sum_{j=1}^{2} L_{ij}\Phi_j(z_j)\right]. \tag{6d}$$

Here, $(\,)'$ designates the derivative with respect to the associated arguments, and **A** and **L** are two matrices whose elements depend upon the elastic constants as

$$\mathbf{A} = \begin{bmatrix} (s_{11}\mu_1^2 + s_{12}) & (s_{11}\mu_2^2 + s_{12}) \\ (s_{12}\mu_1 + s_{22}/\mu_1) & (s_{12}\mu_2 + s_{22}/\mu_2) \end{bmatrix} \tag{7a}$$

$$\mathbf{L} = \begin{bmatrix} -\mu_1 & -\mu_2 \\ 1 & 1 \end{bmatrix}. \tag{7b}$$

2.2 Solution of the Problem. For two aligned orthotropic media, it is possible to define two generalized Dundurs (1968) parameters α and β, which are the only bi-material constants that enter the solution for the problem involving dissimilar materials with prescribed tractions at the boundary. Thus, the solution for the problem under consideration should depend upon λ and ρ for each material and the two bi-material parameters α and β, defined as (Suo, 1988)

$$\alpha = \frac{[\sqrt{(s_{11}s_{22})_2}/\sqrt{(s_{11}s_{22})_1} - 1]}{[\sqrt{(s_{11}s_{22})_2}/\sqrt{(s_{11}s_{22})_1} + 1]} \tag{8a}$$

$$\beta = \frac{[\sqrt{s_{11}s_{22}} + s_{12}]_2 - [\sqrt{s_{11}s_{22}} + s_{12}]_1}{\sqrt{H_{11}H_{22}}} \tag{8b}$$

where

$$H_{11} = [2n\lambda^{1/4}\sqrt{s_{11}s_{22}}]_1 + [2n\lambda^{1/4}\sqrt{s_{11}s_{22}}]_2 \tag{8c}$$

$$H_{22} = [2n\lambda^{-1/4}\sqrt{s_{11}s_{22}}]_1 + [2n\lambda^{-1/4}\sqrt{s_{11}s_{22}}]_2. \tag{8d}$$

2.3 Engineering Approximations. Suo and Hutchinson

(1989) have pointed out that for the case of a crack lying along the interface, the Dundurs parameter β is responsible for the pathological oscillatory behavior of the stresses near the crack tip. Due to the weak dependence of stresses on β and the fact that β itself only takes on small values for most practical cases of interest, Suo and Hutchinson (1989) have suggested that β could be equated to zero to establish a useful engineering approach to such interface problems. However, in the present class of problems discussed here where the cracks terminate at right angles to the interface, there is no oscillatory behavior associated with the nonzero values of β. Therefore, the development of the entire stress field in terms of finite β, without equating it *a priori* to zero, is meaningful. In most of the practical cases the variation of β is between $-1/4$ and $1/4$. The variation of the normal stress at the interface as a function of α could then be up to 25 percent for the above range of β values, which could be relevant since this is the stress component that directly affects the interface delamination criterion. Fortunately, the greatest sensitivity of the normal stress at the interface is restricted to values of α in the range of $|\alpha| > 0.5$, where very few of the practical bi-material combinations fall. Hence, for operational purposes, we have taken $\beta = 0$ in discussing specific cases, because this simplifies the computations without much loss of accuracy. Specifically, neglecting β diagonalizes the bi-material matrix **H** presented in the Appendix, whose elements depend only on the bi-material constants.

With $\beta = 0$, it is possible to further re-scale the x-axis to collapse the dependence of the solution on λ_1 and λ_2 into a new parameter Λ ($[\lambda_1/\lambda_2]^{1/4}$), thereby reducing the number of independent parameters characterizing the solution to 4, i.e., ρ_1, ρ_2, Λ, and the Dundurs parameter α.

2.4 Method of Solution. The semi-infinite crack is simulated as an array of continuously distributed edge dislocations along the negative y-axis, with components $b_1(y_o)$ at $y = y_o$ as shown in Fig. 1(b). The traction-free condition on the plane of the crack with the dislocation distribution results in the integral equation

$$\sigma_{11} = 0 = \frac{1}{8\pi m_2 n_2 s_2}\,\mathrm{Re}\left[\int_{-\infty}^{0}\left[\frac{[-\mu_1^{II}C_{11}^*]}{y+y_o}+\frac{[\mu_2^{II}C_{22}^*]}{y+y_o}-\frac{[\mu_2^{II}C_{21}^*]}{y+(\mu_1^{II}/\mu_2^{II})y_o}+\frac{[\mu_1^{II}C_{12}^*]}{y+(\mu_2^{II}/\mu_1^{II})y_o}\right]b_1'(y_o)d(iy_o)\right]$$
$$+\frac{1}{8\pi m_2 n_2 s_2}\,\mathrm{Re}\left[\int_{-\infty}^{0}\left[\frac{[\mu_1^{II}-\mu_2^{II}]}{y-y_o}\right]b_1'(y_o)d(iy_o)\right] \quad (9)$$

where $s_2 = (\sqrt{s_{11}s_{22}})_2$, and m and n are the same as defined before in Eq. (5d), and $b_1'(y_o)d(iy_o)$ is the local Burgers vector density of the continuous distribution of dislocation between y_o and $y_o + dy_o$. The constants C_{ij}^* are coefficients of a matrix depending upon ρ_1, ρ_2, Λ, and α characterizing the corresponding kernel solution of an edge dislocation at $(0, y_o)$ near the bi-material interface as shown in Fig. 1(c). The superscript II on μ's and the subscript 2 on m, n, and s is chosen to refer to medium 2, which in turn hosts the crack. The constant β influences the solution only through the C_{ij}^*'s. The complete kernel solution along with the expressions for C_{ij}^*'s are given in the Appendix. In this class of problems the radial dependence of the stresses is of the form

$$\sigma\alpha(r)^{\gamma}, \quad (10)$$

where γ is the strength of the singularity. Therefore, each integral in Eq. (9) can be evaluated in a closed form leading to the following characteristic equation

$$[t_2^{II}C_{22}-t_1^{II}C_{11}]+t_1^{II}C_{12}\left(\frac{t_1^{II}}{t_2^{II}}\right)^{(\gamma+1)}-C_{21}t_2^{II}\left(\frac{t_2^{II}}{t_1^{II}}\right)^{(\gamma+1)}-\cos[\pi\gamma(t_1^{II}-t_2^{II})]=0, \quad (11)$$

where $t_1 = n + m$, $t_2 = n - m$. Since the C_{ij}^*'s are known from the kernel solution, the strength of the singularity, γ, can be determined for a given material pair (thereby fixing μ_1 and μ_2) from Eq. (11).

2.5 Results for Stresses. Knowing γ, the stress obtained from the kernel solution can be integrated over the complex domain to determine the expressions for stresses in the two media. The resulting stresses in the vicinity of the interface crack are obtained in closed form

$$\tilde{\sigma}_{11}^{I}(0\text{ deg}) = \sin(\pi\gamma)\left\{\begin{matrix}[-C_{11}(t_1^I)^2(t_1^{II})^{-(\gamma+1)}]+[C_{12}(t_1^I)^2(t_2^{II})^{(\gamma+1)}]\\ -[C_{21}(t_2^I)^2(t_1^{II})^{-(\gamma+1)}]+[C_{22}(t_2^I)^2(t_2^{II})^{-(\gamma+1)}]\end{matrix}\right\} \quad (12a)$$

$$\tilde{\sigma}_{22}^{I}(0\text{ deg}) = \tilde{\sigma}_{22}^{II}(0\text{ deg}) = \sin(\pi\gamma)\left\{\begin{matrix}[C_{11}(t_1^{II})^{-(\gamma+1)}]-[C_{12}(t_2^{II})^{-(\gamma+1)}]\\ +[C_{21}(t_1^{II})^{-(\gamma+1)}]-[C_{22}(t_2^{II})^{-(\gamma+1)}]\end{matrix}\right\} \quad (12b)$$

$$\tilde{\sigma}_{12}^{I}(0\text{ deg}) = \tilde{\sigma}_{12}^{II}(0\text{ deg}) = -(\cos(\pi\gamma)-1)\left\{\begin{matrix}-[C_{11}t_1^I(t_1^{II})^{-(\gamma+1)}]+[C_{12}t_1^I(t_2^{II})^{-(\gamma+1)}]\\ -[C_{21}t_2^I(t_1^{II})^{-(\gamma+1)}]+[C_{22}t_2^I(t_2^{II})^{-(\gamma+1)}]\end{matrix}\right\} \quad (12c)$$

$$\tilde{\sigma}_{11}^{II}(0\text{ deg}) = -\sin(\pi\gamma)\left\{\begin{matrix}[C_{11}(t_1^{II})^2(t_1^{II})^{-(\gamma+1)}]-[C_{12}(t_1^{II})^2(t_2^{II})^{-(\gamma+1)}]\\ +[C_{21}(t_2^{II})^2(t_1^{II})^{-(\gamma+1)}]-[C_{22}(t_2^{II})^2(t_2^{II})^{-(\gamma+1)}]\end{matrix}\right\} + \sin(\pi\gamma)[-(t_1^{II})^{(1-\gamma)}+(t_2^{II})^{(1-\gamma)}] \quad (12d)$$

$$\tilde{\sigma}_{11}^{I}(90\text{ deg}) = 2\sin(\pi\gamma/2)\times\left\{\begin{matrix}[-C_{11}(t_1^I)^{(2+\gamma)}(t_1^{II})^{-(\gamma+1)}]+[C_{12}(t_1^I)^{(2+\gamma)}(t_2^{II})^{-(\gamma+1)}]\\ -[C_{21}(t_2^I)^{(2+\gamma)}(t_1^{II})^{-(\gamma+1)}]+[C_{22}(t_2^I)^{(2+\gamma)}(t_2^{II})^{-(\gamma+1)}]\end{matrix}\right\} \quad (12e)$$

$$\tilde{\sigma}_{22}^{I}(90\text{ deg}) = 2\sin(\pi\gamma/2)\left\{\begin{matrix}[C_{11}(t_1^I)^{\gamma}(t_1^{II})^{-(\gamma+1)}]-[C_{12}(t_1^I)^{\gamma}(t_2^{II})^{-(\gamma+1)}]\\ +[C_{21}(t_2^I)^{\gamma}(t_1^{II})^{-(\gamma+1)}]-[C_{22}(t_2^I)^{\gamma}(t_2^{II})^{-(\gamma+1)}]\end{matrix}\right\} \quad (12f)$$

in the Appendix. Finally, the actual stresses σ_{ij} are obtained from

$$\sigma_{ij} = \left[\frac{K(2\pi r)^{\gamma}}{8n_2s_2m_2}\right]\tilde{\sigma}_{ij} \quad (13)$$

where K is the generalized stress intensity factor having the dimensions (stress/(length)$^{\gamma}$) and is defined on the basis of

$$K(2\pi r)\gamma = \sigma_{xx}(\theta = 90\text{ deg}, r), \quad (14)$$

so as to recover the conventional stress intensity factor for cracks in an infinite homogeneous isotropic material. The expressions for stresses given via Eqs. (12) and (13) can be further normalized in terms of this stress intensity factor as defined above, as

$$\frac{\sigma_{ij}}{K(2\pi r)^{\gamma}} = \bar{\sigma}_{ij}. \quad (15)$$

Thus, for a given bi-material pair, the stress ratios can be

calculated using the above expressions. The explicit expressions for C_{ij}'s in terms of β and other elastic constants of the two media are given in the Appendix. In the next section we work out the stress ratios for the case of a crack in a SiC coating terminating perpendicularly on an interface between it and a Pitch-55 fiber.

2.6 Crack Deflection Criterion for the SiC Coating/Pitch-55 Fiber Interface. Since the present investigation was motivated by the specific goal to tailor the properties of an interface between a coating such as SiC and a fiber such as Pitch-55, in a composite with a matrix such as aluminum, we calculate here the crack deflection criterion specifically for a crack in a SiC coating terminating perpendicularly on a Pitch-55 fiber. The fiber is modelled as a homogeneous orthotropic material with the elastic constants given in Table 1, while the SiC coating is considered as isotropic with elastic constants also shown in Table 1. For a pair consisting of high modulus SiC coating and Pitch-55 fiber, the bi-material parameters are: $\alpha = -0.4$; $\beta = 0.04$, $\rho_1 = 2.43$, $\lambda_1 = 0.034$, $\rho_2 = 1$ and $\lambda_2 = 1$ (SiC coating is considered to be isotropic as stated above). For these material constants, the singularity exponent γ is equal to -0.46, as determined from Eq. (11), and the values of the various crack-tip stresses in the fiber and the coating are given in Table 2. The stresses are normalized as discussed above.

The stress acting across the interface, particularly the normal component of it, is of interest for the determination of the crack deflection criterion discussed in Section 1. Since the normal stress in Table 2 is normalized with respect to the axial stress in the fiber, therefore, the crack deflection criterion is satisfied if the ratio of σ_i^*/σ_f^* is less than 0.136 where σ_i^* and σ_f^* are the tensile cohesive strengths of the interface and the fiber, respectively. The average strength of the Pitch-55 fiber was determined from independent experiments to be 1.2 GPa (Zhang et al., 1990). Hence, in order to deflect the crack along the interface, the interface tensile strength should be less than 163 MPa. This calculation is specific to the above pair. Coatings of SiC deposited under different conditions can have different elastic properties and interface strength when deposited on Pitch-55 fibers. Therefore, to cope with a wide range of possibilities and with other general coating/fiber systems, we develop generalized interface delamination charts—albeit with operational simplifications.

Table 1 Elastic constants for the Pitch-55 fiber and SiC coating

material	E_{11}	E_{22}	μ_{12}	ν_{12}
Pitch-55 fiber	380	13	-	0.45
SiC Coating (Isotropic, high IBE)	300	300	115.4	0.3
SiC Coating (Isotropic, low IBE)	16	16	6.5	0.3

IBE: ion beam energy

Table 2 Normalized stress components at an interface between a anisotropic Pitch-55 fiber and SiC coating

Normalized Components	Calculated Stress Ratios
$\sigma_{xx}(\pi/2)^I/(K(2\pi r)^\gamma)$	1.000
$\sigma_{yy}(\pi/2)^I/(K(2\pi r)^\gamma)$	0.516
$\sigma_{xx}(0)^I/(K(2\pi r)^\gamma)$	1.157
$\sigma_{xx}(0)^{II}/(K(2\pi r)^\gamma)$	4.487
$\sigma_{yy}(0)^I/(K(2\pi r)^\gamma) = \sigma_{yy}(0)^{II}/(K(2\pi r)^\gamma)$	0.136
$\sigma_{xy}(0)^I/(K(2\pi r)^\gamma) = \sigma_{xy}(0)^{II}/(K(2\pi r)^\gamma)$	0.344

3 Generalized Delamination Charts

3.1 Factors Affecting Interface Delamination. The advantage of expressing the solution set in closed form is that the relations given in Section 2.5 can be used to determine the interface stress state for any material pair as demonstrated above for a special case of a SiC/Pitch-55 pair. However, through considerations of wider ranges of properties of bi-material pairs, it can be noted that the stress components are not very sensitive to all the anisotropic constants within certain engineering approximations. In this section, we identify the key anisotropic parameters having major influence on the delamination criterion, for the purpose of constructing generalized delamination charts. While the effect of the Dundurs parameter β has already been identified as being relatively weak for practical bi-material pairs, the effect of ρ and λ on the delamination condition must be assessed. Typical values of ρ and λ for some engineering materials are assembled in Table 3 (Suo, 1988). We note that while the values of λ change quite significantly, those for ρ change much less with increasing degree of anisotropy. For example, for the epoxy matrix/fiber composite with GY70 fibers, the homogenized orthotropic composite will have a value of $1/\lambda = 42$ relative to unity for a reference material with transverse cubic symmetry, while the value of ρ will only be 3.36 relative to unity for a reference material with transverse isotropy. Since the variation in the parameter ρ is relatively little and, as we will see below in Section 3.1.3, the dependence of the stresses on ρ are relatively weak, we will simplify the following discussion considerably by choosing ρ_1 and ρ_2 to be unity. For the case of the cracked component, the choice of $\rho_2 = 1$ is physically acceptable, since the cracked component is often an isotropic coating. For the case of the probed component, the choice of $\rho_1 = 0$ is merely an operational simplification for a usually anisotropic solid without serious sacrifice in accuracy.

3.1.1 Effect of β. Figure 2(*a*, *b*) shows the effect of the variation of β on various normalized (normalized with σ_{xx}^I(90 deg)) stress components for the special case of $\lambda_1 = \lambda_2 = \rho_1 = \rho_2 = 1.0$, i.e., for transverse isotropy in both the materials. Since the magnitude of the axial stress at the interface in medium 2 (i.e., σ_{xx}(0 deg)) is large as compared to the other components, it has been plotted separately in Fig. 2(*b*). The effect of β on most of the important stress components is negligible for practical ranges of β between 1/4 and $-1/4$. However, for certain values of α, the normal stress acting across the interface (σ_{yy}(0 deg) and the transverse stress in the

Table 3 λ and ρ values (Suo, 1989)

material	plane stress		plane strain	
	$1/\lambda$	ρ	$1/\lambda$	ρ
Al (fcc)	1	0.76	1	0.72
Cr (bcc)	1	1.51	1	1.52
Cu (fcc)	1	.02	1	-0.19
Nb (bcc)	1	2.28	1	2.47
ash (LR)	10.5	1.68	7.9	1.88
balsa (LR)	21.0	2.13	17.8	2.29
oak (LR)	2.7	1.16	2.3	1.21
pine (LR)	14.8	1.09	12.1	1.18
boron/epoxy	9.1	6.14	8.3	6.43
S-glass/epoxy	2.4	1.47	2.3	1.51
graphite/epoxy	14.0	2.73	12.8	2.85
aramid/epoxy	17.4	3.49	16.0	3.64
pitch-55 fiber	-	-	29.23	2.43

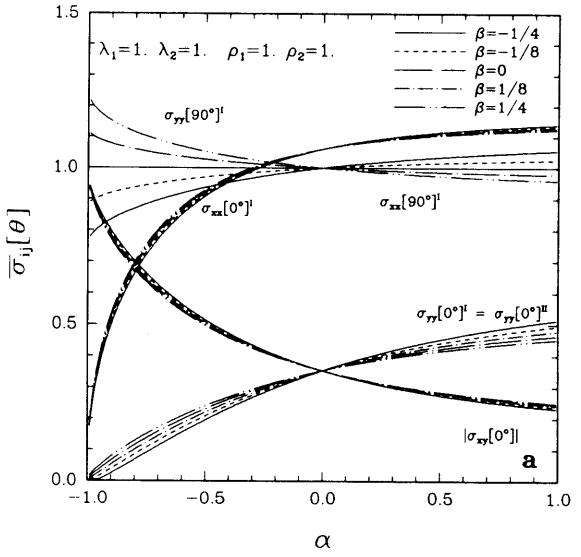

Fig. 2(*a*) Effect of β on normalized stress components

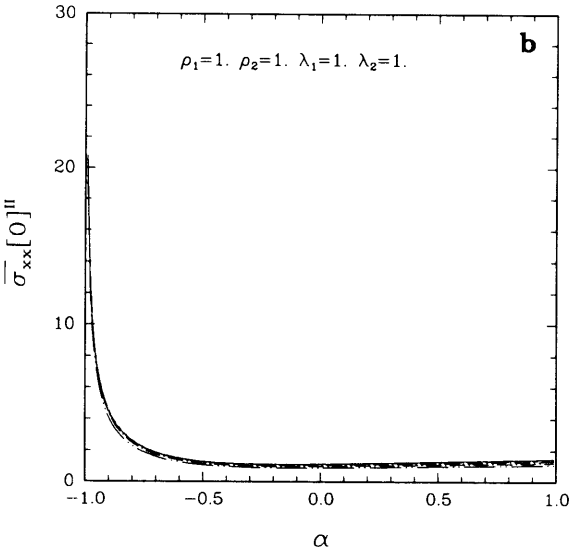

Fig. 2(*b*) σ_{xx} (0 deg) plot in medium II

fiber (σ_{yy}(90 deg)) shows significant dependence on β. The normal stress at the interface is most sensitive to the variation in β for $\alpha < -0.5$. It changes by almost 15 percent for $\alpha = -0.7$ with a corresponding variation in β from $-1/4$ to $1/4$. Thus, for bi-material combinations lying in this sector, the effect of β should be considered. Similarly, the transverse component of stress in the fiber, i.e., σ_{yy}(90 deg) shows a strong dependence on β for values of α in the ranges $\alpha < -0.5$ and $\alpha > 0.6$. Specifically, for $\alpha = -0.9$, σ_{yy}(90 deg) varies by almost 17 percent from that for the $\beta = 0$ case. Such effects may be critical in understanding the transverse behavior of the composite. Nevertheless, if the bi-material pair falls within the sensitive ranges of Dundurs parameters, the dependence on β directly can be calculated by using the expressions for stresses given in Section 2.5. Data for the interdependence of the Dundurs parameters has been explored by Suga et al. (1988) who have discovered that in all the cases considered β depends only weakly on α, and that the associated changes in β are only approximately one tenth of the change in α. Thus, a choice of $\beta = 0$ for arbitrary α provides little compromise in accuracy as Fig. 2(*a*) shows for most of the relevant components of stress. Hence, for the remainder of our discussion, $\beta = 0$ will be chosen. For $\beta = 0$, it is possible to further rescale the x-axis to collapse the dependence on λ_1 and λ_2 into one parameter Λ, thereby reducing the number of independent parameters

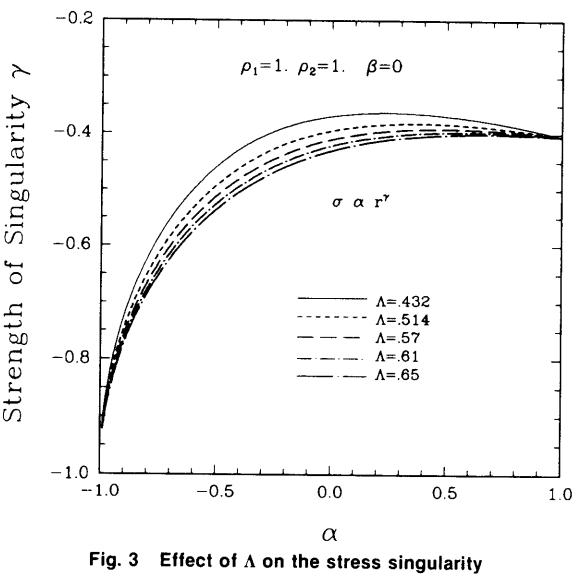

Fig. 3 Effect of Λ on the stress singularity

characterizing the solution to only 4 parameters, i.e., ρ_1, ρ_2, Λ, and α. It is interesting to note that the parameters used to determine solutions presented in Fig. 2(*a*) and (*b*) make both the materials isotropic, albeit still quite different from each other. Thus, these figures give another representation of the earlier solution of Swenson and Rau (1970) presented here in terms of the Dundurs parameters rather than the ratios of moduli and Poisson's ratios.

3.1.2 Effect of Λ. Figure 3 shows the effect of the variation of Λ on the dependence of the stress singularity exponent γ on α for $\rho_1 = \rho_2 = 1.0$ with the qualifications stated in Section 3.1.1. The strength of the singularity exponent is most sensitive to the variation in Λ in the range $-0.75 < \alpha < 0.35$. In this range, the maximum change in singularity exponent is 16 percent (for $\alpha = -0.375$) with an increase in the value of Λ from 0.43 to 0.65. Thus, for certain specific values of α between -0.75 and 0.5, it may become necessary to account for the effect of Λ while calculating the structure of the stress and displacement field if higher accuracy is required. However, for certain ranges of α, i.e., $-1 < \alpha < -0.75$ and $0.5 < \alpha < 1$, the effect of the variation of Λ on the strength of the singularity exponent can be practically ignored. Since all the stress components have the same radial dependence, the effect of Λ on most of the normalized stress components is almost negligible as depicted in Fig. 4, with the exception of σ_{yy}(90 deg)^I; i.e., the normalized stress probing the fiber in the transverse direction is most sensitive to Λ. As shown in Fig. 4, it changes by almost 27 percent for $\alpha = -0.75$. While this stress is of no importance in interface decohesion, it could be of importance in axial delamination of the fiber just ahead of the crack tip in a manner envisioned by Cook and Gordon (1964). The normalized stress components governing the interface delamination in tension (σ_{yy}(0 deg)) and shear (i.e., σ_{xy}(0 deg)) are insensitive to the variation in Λ. Thus, in presenting the interface delamination criteria, the effect of Λ can be largely ignored within engineering approximations. It is, however, important to understand the implications of high normal stresses generated across the fiber for certain values of α on the transverse strength of the composite. Qualitatively, it appears that these high stresses will further intensify the stresses at the interface when the composite is simultaneously loaded in the transverse direction. Results for such stress concentrations were given by Zywicz and Parks (1988) when the composite was loaded only in the transverse direction. Further analysis for the stress concentrations at the interface are required for the case of simultaneous loading of the composite in the axial and the transverse direction.

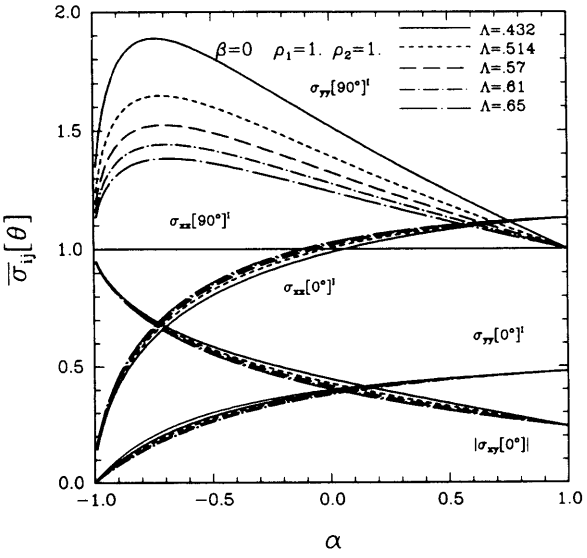

Fig. 4 Effect of Λ on normalized stress components

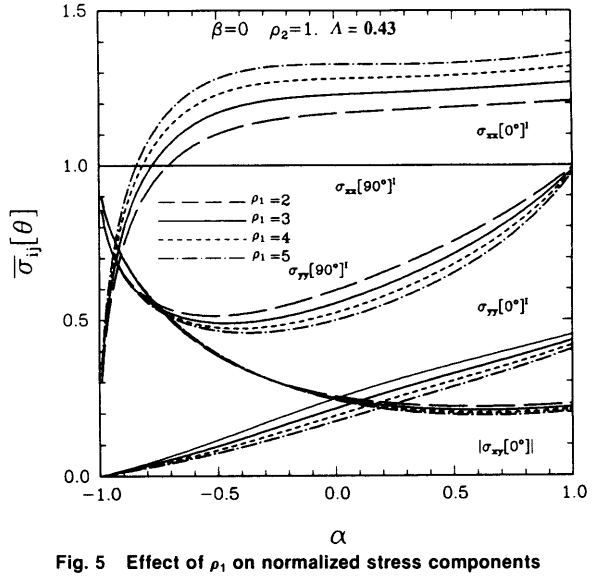

Fig. 5 Effect of ρ_1 on normalized stress components

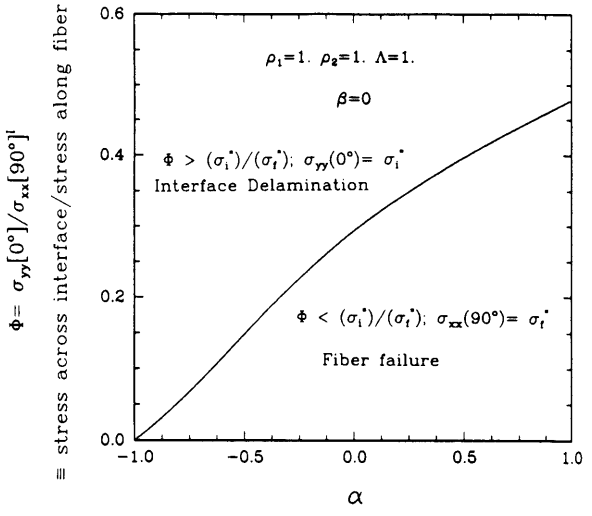

Fig. 6 Generalized interface chart for $\beta = 0$

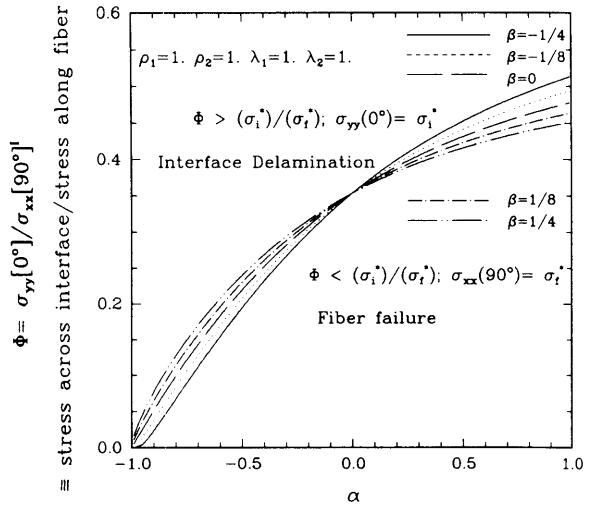

Fig. 7 Generalized interface chart for large values of β

3.1.3 Effect of ρ_1. Since the coatings are usually isotropic, only the effect of the variation of ρ_1 on the various components of normalized stress is studied in this section. Figure 5 shows such effects. Interestingly, all but the shear stress at the interface shows significant dependence on ρ_1.

In conclusion, except for certain ranges of α and β values, the normal stress at the interface is not very sensitive to the variation in ρ_1, Λ, and β from their corresponding isotropic values. Therefore, a generalized delamination chart can be constructed as shown in Fig. 6 for $\beta = 0$ and with ρ_1, ρ_2, and Λ assuming their isotropic values. For material pairs falling in the range where the effect of β is important, Fig. 7 can be used to determine the delamination criterion for a specific value of β. While reading the values from the delamination charts, it is reminded that the cracked component is to be designated as material 2. For exact results, the formulae given in Section 2.5 should be used.

Since the parameters used to determine the stresses that are plotted in Figs. 6 and 7 make each of the two media isotropic, it appears that a generalized crack deflection criterion for a pair of aligned orthotropic solids coincides with that for a pair of isotropic materials, albeit in an approximate manner. This is merely a coincidence. Since the results presented in Figs. 6 and 7 still contain the most important influence of anisotropy through the two Dundurs parameters α and β, it becomes possible to determine the crack deflection criterion for a pair of anisotropic materials by calculating α and β via Eqs. 8(*a*, *b*) in terms of the orthotropic elastic constants. In the absence of such considerations in the existing solution of Swenson and Rau (1970), it is only possible to estimate the crack deflection criterion by defining an effective modulus, which in turn can be taken as an arithmetical or geometrical mean of the orthotropic stiffnesses. In the absence of any formulae accounting for anisotropy, substantial errors can be introduced through such averaging techniques in cases with large differences between the axial and transverse direction elastic properties. In fact, the present developments were motivated because the Pitch-55 fiber has an axial modulus of 380 GPa and a transverse modulus of only 13 GPa.

Although knowledge of these normalized stresses for cracks terminating on the interface should be quite useful for purely elastic behavior, experimental observations on interface delamination (Gupta et al., 1989; Argon et al., 1989) indicate that additional considerations will be necessary when plastic deformation in the fiber accompanies the propagation of the delamination crack. Initial attempts to solve such problems have been made recently by Zywicz and Parks (1990) and Shih and Asaro (1989).

4 Optimizing Toughness and Transverse Strength in Composites With the Delamination Charts

In addition to high toughness by controlled interface delamination, the ability of the composite to sustain high transverse stresses in service is of considerable importance. Unfortunately, maximizing these two properties demand satisfying conflicting requirements on the interface strength. High interface strength is required for the composite to carry high transverse stresses. In contrast, low interface strength is desirable to enhance the toughness of the composite by crack deflection at interfaces. Interestingly, the level of the interface strength required to satisfy the longitudinal delamination criterion can be elevated by an appropriate choice for the elastic properties of the coating or the fiber and thereby permit the composite to support higher transverse operating stresses. Specifically, with respect to the delamination chart shown in Fig. 6 or 7, the bi-material properties can be chosen to push α towards extreme positive values. Since α depends on the relative elastic properties of the two media (see Eq. (8*a*)), this could be achieved in several ways. First, in composite systems where protective coatings are deposited on the fiber surface by using the plasma CVD technique, it is possible to control the coating modulus by controlling the deposition conditions (Landis, 1987). Second, it is also possible to use different types of carbon fibers with different elastic properties.

Table 4 shows the calculated values of the maximum permissible interface strength required for the operation of the crack deflection criterion for various coating/fiber interfaces. These interface values are calculated in the following way: Using the known elastic compliances for various materials, the value of α is calculated via Eq. (8*a*). For these values of α, the ratio σ_i^*/σ_f^* is determined from Fig. 6. Finally, taking the value of σ_f^* either from the manufacturer's handbooks or from the experiments of Zhang et al. (1990) in the case of Pitch-55 fiber, the permissible peak value for the interface strength is calculated. The transverse strength of the composite is then estimated by assuming a transverse interface stress concentration; e.g., 2.4 as determined by Zywicz and Parks (1988) for a hexagonal array of Pitch-55 carbon fibers surrounded by an aluminum matrix. Table 4 shows that for the case of low energy ion beam SiC coated Pitch-100 fiber the maximum level of the interface strength can be dramatically increased to 0.390 GPa. With the Al/Nicalon composite system, it appears that transverse strength values as high as 0.47 GPa can be achieved using the same transverse stress concentration factor of 2.4 determined for the Pitch-55/aluminum case.

Thus, it is possible to maximize both the transverse strength and the toughness in fiber composites with a judicious choice of the coating/fiber/matrix system based on the delamination charts given here.

5 Discussion

The strategy of deflecting cracks along interfaces to enhance the toughness of fiber composites is under active study (see, e.g., Argon et al., 1989; Evans, 1989). The first step in this attempt is to establish the crack deflection criterion. For composites with anisotropic high modulus carbon fibers, it becomes necessary to incorporate the elastic anisotropy of the fiber in these deflection analyses. Such analysis, with two aligned orthotropic media, has been considered here. The stress and deformation fields derived for such cases are shown to depend on the material parameters λ and ρ for the two media and the two bi-material constants α and β. The delamination criterion is insensitive to λ, ρ, Λ, and β over practical ranges of these material parameters. Thus, generalized delamination charts can be constructed as a function of the main bi-material constant α, which characterizes the elastic dissimilarity of the two media. Using these charts, it is possible to determine the desired level of interface strength required in composite manufacturing in order to enhance its overall toughness. Furthermore, these charts can be used for the fiber/coating or the fiber/matrix or the matrix/coating interface, depending upon which interface is of critical interest to achieve the crack deflection process.

Table 4 Maximum allowable interface strength for interface delamination.

Composite System (Matrix or Coating/Fiber)	α	Required Interface Strength (GPa)	Calculated Transverse Strength (GPa)
Al/P-55	0.001	0.475	0.197
Al/P-100	0.153	0.726	0.300
SiC (HBE**)/P-55	-0.605	0.209	0.086
SiC (LBE*)/P-55	0.574	0.836	0.350
SiC (HBE)/P-100	-0.499	0.330	0.136
SiC (LBE)/P-100	0.668	0.946	0.390
SiC (LBE)/Alumina	0.904	0.788	0.326
Al/Nicalon	0.468	1.148	0.470
TiC/Alumina	-0.085	0.508	0.210

** SiC deposited with high ion beam energy.

* SiC deposited with low ion beam energy

Acknowledgment

This research was supported by the Office of Naval Research under contract N00014-85-K-0645. For this support, we are grateful to Dr. S. Fishman of that agency. Useful discussions with Prof. J. W. Hutchinson are also acknowledged. We are also grateful to Dr. James Cornie for providing the information used in constructing Table 4.

References

Argon, A. S., Gupta, V., Landis, H. S., and Cornie, J. A., 1989, "Intrinsic Toughness of Interfaces Between SiC Coatings and Substrates of Si and C Fibers," *Journal of Materials Science*, Vol. 24, pp. 1207–1218.

Cook, J., and Gordon, J. E., 1964, "A Mechanism for the Control of Crack Propagation in all Brittle Systems," *Proceedings of the Royal Society, London*, Vol. A282, pp. 508–520.

Dundurs, J., 1968, "Elastic Interaction of Dislocations with Inhomogeneities," *Mathematical Theory of Dislocations*, ASME, New York, pp. 70–115.

Erdogan, F., 1972, "Fracture Problems in Composite Materials," *Engineering Fracture Mechanics*, Vol. 4, No. 4, pp. 811–840.

Erdogan, F., and Biricikoglu, V., 1973, "Two Bonded Half Planes with a Crack Going Through an Interface," *International Journal of Engineering Science*, Vol. 11, pp. 745–766.

Eshelby, J. D., Read, W. T., and Shockley, W., 1953, "Anisotropic Elasticity with Applications to Dislocation Theory," *Acta Metallurgica*, Vol. 1, pp. 251–259.

Evans, A. G., 1989, "The Mechanical Performance of Fiber-Reinforced Ceramic Matrix Composites," *Materials Science and Engineering*, Vol. A107, pp. 227–239.

Gupta, V., Argon, A. S., and Cornie, J. A., 1989, "Interfaces with Controlled Toughness as Mechanical Fuses to Isolate Fiber from Damage," *Journal of Materials Science*, Vol. 24, pp. 2031–2040.

Landis, H. S., 1987, "Amorphous Hydrogenated SiC by Plasma Enhanced Chemical Vapor Deposition for Metal Matrix Composite Applications," Ph.D. Thesis, Department of Materials Science and Engineering, M.I.T., Cambridge, Ma.

Lekhnitskii, S. G., 1963, *Theory of Elasticity of an Anisotropic Body*, Holden-Day, San Francisco.

Shih, C. F., and Asaro, R. J., 1989, "Elastic-Plastic Analysis of a Collinear Array of Cracks on a Bi-material Interface," *Materials Science and Engineering*, Vol. A107, pp. 227–239.

Stroh, A. N., 1958, "Dislocations and Cracks in Anisotropic Elasticity," *Philosophical Magazine*, Vol. 3, pp. 625–646.

Suga, T., Elssner, E., and Schmander, S., 1988, "Composite Parameters and Mechanical Compatibility of Mechanical Joints," *Journal of Composite Materials*, Vol. 22, pp. 917–934.

Suo, Z., 1989, "Singularities Interacting with Interfaces and Cracks," *International Journal of Solids and Structures*, Vol. 25, No. 10, pp. 1133–1142.

Suo, Z., 1990, "Delamination Specimens for Orthotropic Materials," ASME JOURNAL OF APPLIED MECHANICS, Vol. 57, pp. 627–634.

Suo, Z., and Hutchinson, J. W., 1989, "Sandwich Test Specimens for Meas-

uring Interface Crack Toughness," *Materials Science and Engineering*, Vol. A107, pp. 135–143.

Swenson, D. O., and Rau, C. A., Jr., 1970, "The Stress Distribution Around a Crack Perpendicular to an Interface Between Materials," *International Journal of Fracture Mechanics*, Vol. 6, pp. 357–360.

Ting, T. C. T., and Hoang, P. H., 1984, "Singularities at the Tip of a Crack Normal to the Interface of an Anisotropic Layered Composite," *International Journal of Solids and Structures*, Vol. 20, No. 5, pp. 439–454.

Zak, A. K., and Williams, M. L., 1963, "Crack Point Singularities at a Bi-material Interface," ASME JOURNAL OF APPLIED MECHANICS, Vol. 30, pp. 142–143.

Zhang, G-D., Feng, F. R., Li, Q., Blucher, J. T., and Cornie, J. A., 1990, "Control of Interface Reactions Between P-55 Fibers and Aluminum Alloy Matrices during Pressure Infiltration Processing," *Controlled Interfaces in Composite Materials, Proceedings of the International Conference on Composite Interfaces-III*, H. Ishida, ed., Elsevier, N.Y., pp. 343–357.

Zywicz, E., and Parks, D. M., 1988, "Thermo Viscous Plastic Residual Stresses in Metal Matrix Composites," *Composite Science and Technology*, Vol. 33, pp. 295–315.

Zywicz, E., and Parks, D. M., 1990, "Elastic-Plastic Analysis of Frictionless Contact at Interfacial Crack Tips," *International Journal of Fracture*, Vol. 42, pp. 129–143.

APPENDIX

In Section 2.4, the solution of an edge dislocation embedded at $(0, y_o)$ in a composite of two aligned orthotropic material (Fig. 1*c*) is used as the kernel of the integral equation. This solution is constructed in this Appendix using the fundamental solution of a dislocation in an infinite homogeneous orthotropic medium.

The potential function for an edge dislocation with Burger vector b_1 at the point $(0, y_o)$ in an infinite homogeneous orthotropic body with the principal axis along the x and y axes are given by (Eshelby et al., 1953)

$$\Phi_{jo}(Z) = W_j \ln(Z - S_j),\ S_j = \mu_j y_o. \tag{A1}$$

where the suffix "o" is attached to the potential to indicate that the solution is for the infinite body.

$$W_1 = \frac{1}{[\mu_1^{II} - \mu_2^{II}]}\,[-B_1]$$
$$W_2 = \frac{1}{[\mu_1^{II} - \mu_2^{II}]}\,[B_1] \tag{A2}$$

where

$$B_1 = \frac{b_1}{8\pi n_2 s_2 m_2} \tag{A3}$$

μ_1^{II} and μ_2^{II} are the roots of the characteristic Eq. (4) defined in Section 2.2 and m, n, and s are same as defined before in Eqs. (5*a–d*) and Section 2.4. Now, the potentials for the interaction of an edge dislocation with the interface (Fig. 1) can be obtained in terms of $\Phi_{jo}(z)$ by invoking the standard analytical continuation arguments, along with the continuity of tractions and displacements along the interface, as described by Suo (1989). The solution for the two media can be written as

$$\Phi(z) = \phi^1(z),\ z\epsilon 1 \tag{A4a}$$
$$\Phi(z) = \Phi^2(z) + \Phi_o(z),\ z\epsilon 2 \tag{A4b}$$
$$\Phi^1(z) = \mathbf{C}\Phi_o(z) \tag{A4c}$$
$$\mathbf{C} = \mathbf{L}_1^{-1}\mathbf{H}^{-1}(\overline{\mathbf{B}}_2 + \mathbf{B}_2)\mathbf{L}_2,\ z\epsilon 1 \tag{A4d}$$
$$\Phi^2(z) = \mathbf{G}\overline{\Phi}_o(z) \tag{A4e}$$
$$\mathbf{G} = \mathbf{L}_2^{-1}\overline{\mathbf{H}}^{-1}(\overline{\mathbf{B}}_2 - \mathbf{B}_1)\overline{\mathbf{L}}_2,\ z\epsilon 2 \tag{A4f}$$

where $(\bar{\ })$ denotes the complex conjugation and the subscripts on the matrix are used to indicate the two materials. The matrix $\mathbf{B}$ is a positive definite Hermitian matrix (Stroh, 1958),

$$\mathbf{B} = i\mathbf{A}\mathbf{L}^{-1} \tag{A5}$$

where $\mathbf{A}$ and $\mathbf{L}$ are defined in Section 2.2. Here, $i = \sqrt{-1}$. $\mathbf{H}$ is a positive definite Hermitian matrix defined as

$$\mathbf{H} = \mathbf{B}_1 + \overline{\mathbf{B}}_2. \tag{A6a}$$

Physically, the $\mathbf{H}$ matrix includes the bi-material effects, and hence its element involves the Dundurs parameters α and β. This matrix can be written explicitly as

$$\mathbf{H} = \begin{bmatrix} H_{11} & -i\beta\sqrt{H_{11}H_{22}} \\ i\beta\sqrt{H_{11}H_{22}} & H_{22} \end{bmatrix} \tag{A6b}$$

$$H_{11} = [2n\lambda^{1/4}\sqrt{s_{11}s_{22}}]_1 + [2n\lambda^{1/4}\sqrt{s_{11}s_{22}}]_2 \tag{A6c}$$

$$H_{22} = [2n\lambda^{-1/4}\sqrt{s_{11}s_{22}}]_1 + [2n\lambda^{-1/4}\sqrt{s_{11}s_{22}}]_2 \tag{A6d}$$

$$\sqrt{H_{11}H_{22}}\beta = [\sqrt{s_{11}s_{22}} + s_{12}]_1 - [\sqrt{s_{11}s_{22}} + s_{12}]_2. \tag{A6e}$$

Here, β is a generalization of the Dundurs (1968) parameter. $\beta = 0$ will diagonalize the matrix $\mathbf{H}$ and reduces the extent of matrix algebra. Using Eq. (A4) and Φ_o from Eq. (A1), the potentials for the problem depicted in Fig. 1 can be derived. Once the potentials are known, stresses and displacements can be computed using Eqs. 6(*a–d*). The complete normalized stresses at the interface are given by:

$$\tilde{\sigma}_{11}^I = b_1\left\{\frac{[C_{11}(t_1^I)^2 t_1^{II} y_o]}{[x^2 + (y_o t_1^{II})^2]} - \frac{[C_{12}(t_1^{II})^2 t_2^{II} y_o]}{[x^2 + (y_o t_2^{II})^2]} + \frac{[C_{21}(t_2^I)^2 t_1^{II} y_o]}{[x^2 + (y_o t_1^{II})^2]} - \frac{[C_{22}(t_2^I)^2 t_2^{II} y_o]}{[x^2 + (y_o t_2^{II})^2]}\right\} \tag{A7a}$$

$$\tilde{\sigma}_{12}^I = b_1\left\{\frac{[C_{11} t_1^I x]}{[x^2 + (y_o t_1^{II})^2]} - \frac{[C_{12} t_1^I x]}{[x^2 + (y_o t_2^{II})^2]} + \frac{[C_{21} t_2^I x]}{[x^2 + (y_o t_1^{II})^2]} - \frac{[C_{22} t_2^I x]}{[x^2 + (y_o t_2^{II})^2]}\right\} \tag{A7b}$$

$$\tilde{\sigma}_{22}^I = -b_1\left\{\frac{[C_{11} t_1^{II} y_o]}{[x^2 + (y_o t_1^{II})^2]} + \frac{[C_{12} t_2^{II} y_o]}{[x^2 + (y_o t_2^{II})^2} - \frac{[C_{21} t_1^{II} y_o]}{[x^2 + (y_o t_1^{II})^2]} + \frac{[C_{22} t_2^{II} y_o]}{[x^2 + (y_o t_2^{II})^2]}\right\} \tag{A7c}$$

$$\tilde{\sigma}_{11}^{II} = b_1\left\{\frac{[C_{11}^*(t_1^{II})^2 t_1^{II} y_o]}{[x^2 + (y_o t_1^{II})^2]} - \frac{[C_{12}^*(t_1^{II})^2 t_2^{II} y_o]}{[x^2 + (y_o t_2^{II})^2]} + \frac{[C_{21}^*(t_2^{II})^2 t_1^{II} y_o]}{[x^2 + (y_o t_1^{II})^2]} - \frac{[C_{22}^*(t_2^{II})^2 t_2^{II} y_o]}{[x^2 + (y_o t_2^{II})^2]} - \frac{[(t_2^{II})^2 t_2^{II} y_o]}{[x^2 + (y_o t_2^{II})^2]} + \frac{[(t_1^{II})^2 t_1^{II} y_o]}{[x^2 + (y_o t_1^{II})^2]}\right\} \tag{A7d}$$

The component of normalized stresses in front of the crack tip in medium I can be written as:

$$\tilde{\sigma}_{11}^I = -b_1\left\{-\frac{[C_{11} t_1^I]}{[y - y_o(t_1^{II}/t_1^I)]} + \frac{[C_{12} t_1^I]}{[y - y_o(t_2^{II}/t_1^I)]} - \frac{[C_{21} t_2^I]}{[y - y_o(t_1^{II}/t_2^I)]} + \frac{[C_{22} t_2^I]}{[y - y_o(t_2^{II}/t_2^I)]}\right\} \tag{A7e}$$

$$\tilde{\sigma}_{22}^I = b_1\left\{\frac{[C_{11}]}{t_1^I[y - y_o(t_1^{II}/t_1^I)]} - \frac{[C_{12}]}{t_1^I[y - y_o(t_2^{II}/t_1^I)]} + \frac{[C_{21}]}{t_2^I[y - y_o(t_1^{II}/t_2^I)]} - \frac{[C_{22}]}{t_2^I[y - y_o(t_2^{II}/t_2^I)]}\right\} \tag{A7f}$$

where

$$\sigma_{ij} = \left[\frac{1}{8\pi n_2 s_2 m_2}\right]\tilde{\sigma}_{ij}. \tag{A7g}$$

Here, C_{ij} and C^*_{ij} are, respectively, the elements of the matrices **C** and **G** as defined in Eq. (A4). The expressions for C_{ij} and C^*_{ij} are given by

$$C_{11}=\frac{1}{(t_2^I-t_1^I)}\left[-Q_1t_1^{II}+Q_2+t_2^I(Q_3t_1^{II}+Q_4)\right] \quad (A8a)$$

$$C_{12}=\frac{1}{(t_2^I-t_1^I)}\left[-Q_1t_2^{II}+Q_2+t_2^I(Q_3t_2^{II}+Q_4)\right] \quad (A8b)$$

$$C_{21}=\frac{1}{(t_2^I-t_1^I)}\left[Q_1t_1^{II}-Q_2-t_1^I(Q_3t_1^{II}+Q_4)\right] \quad (A8c)$$

$$C_{22}=\frac{1}{(t_2^I-t_1^I)}\left[Q_1t_2^{II}-Q_2-t_1^I(Q_3t_2^{II}+Q_4)\right] \quad (A8d)$$

$$C^*_{11}=\frac{1}{(t_2^{II}-t_1^{II})}\left[Q_1^*t_1^{II}-Q_2^*+t_2^{II}(Q_3^*t_1^{II}+Q_4^*)\right] \quad (A8e)$$

$$C^*_{12}=\frac{1}{(t_2^{II}-t_1^{II})}\left[Q_1^*t_2^{II}-Q_2^*+t_2^{II}(Q_3^*t_2^{II}+Q_4^*)\right] \quad (A8f)$$

$$C^*_{21}=\frac{1}{(t_2^{II}-t_1^{II})}\left[-Q_1^*t_1^{II}+Q_2^*-t_1^{II}(Q_3^*t_1^{II}+Q_4^*)\right] \quad (A8g)$$

$$C^*_{22}=\frac{1}{(t_2^{II}-t_1^{II})}\left[-Q_1^*t_2^{II}+Q_2^*-t_1^{II}(Q_3^*t_2^{II}+Q_4^*)\right] \quad (A8h)$$

where Q_1 and Q_1^* are used to write the expressions for C_{ij} and C^*_{ij} in compact form. The expressions for Q_1 and Q_1^* depend only on the elastic constants of the two media and are given by

$$Q_1=\frac{2\Sigma}{\left[\left(\frac{n_1}{n_2}\right)\Lambda+\Sigma\right](1-\beta^2)} \quad (A9a)$$

$$Q_2=\frac{\beta}{(1-\beta^2)}\times\left[\frac{2}{\sqrt{\left[\frac{1}{\Sigma}\left(\frac{n_1}{n_2}\right)(\lambda_1\lambda_2)^{1/4}+\lambda_2^{1/2}\right]\left[\frac{n_1}{n_2}\left(\frac{1}{\Lambda\Sigma}\right)+1\right]}}\right] \quad (A9b)$$

$$Q_3=\frac{-\beta}{(1-\beta^2)}\times\left[\frac{2}{\sqrt{\left[\frac{1}{\Sigma}\left(\frac{n_1}{n_2}\right)(\lambda_1\lambda_2)^{-1/4}+\lambda_2^{-1/2}\right]\left[\frac{n_1}{n_2}\left(\frac{\Lambda}{\Sigma}\right)+1\right]}}\right] \quad (A9c)$$

$$Q_4=\frac{2\Sigma\Lambda}{\left[\left(\frac{n_1}{n_2}\right)+\Lambda\Sigma\right](1-\beta^2)} \quad (A9d)$$

$$Q_1^*=\frac{1}{(H_{11}(1-\beta^2))}\left[(2n_2s_2\lambda_2^{1/4})-(2n_1s_1\lambda_1^{1/4})\right]+\frac{\beta^2}{(1-\beta^2)} \quad (A9e)$$

$$Q_2^*=\frac{\beta}{(\sqrt{H_{11}H_{22}}(1-\beta^2))}\left[(2n_2s_2\lambda_2^{-1/4})-(2n_1s_1\lambda_1^{-1/4})\right]+\frac{\beta}{(1-\beta^2)}\left(\sqrt{\frac{H_{22}}{H_{11}}}\right) \quad (A9f)$$

$$Q_3^*=\frac{\beta}{(\sqrt{H_{11}H_{22}}(1-\beta^2))}\left[(2n_2s_2\lambda_2^{1/4})-(2n_1s_1\lambda_1^{1/4})\right]+\left[\frac{\beta}{(1-\beta^2)}\left(\sqrt{\frac{H_{11}}{H_{22}}}\right)\right] \quad (A9g)$$

$$Q_4^*=\frac{1}{(H_{22}(1-\beta^2))}\left[2n_2s_2\lambda_2^{-1/4})-(2n_1s_1\lambda_1^{-1/4})\right]+\frac{\beta^2}{(1-\beta^2)}. \quad (A9h)$$

Here

$$\Lambda=\left(\frac{\lambda_1}{\lambda^2}\right)^{1/4} \quad (A9i)$$

$$\Sigma=\frac{s_2}{s_1},\ s_1=(\sqrt{s_{11}s_{22}})_1 \text{ and } s_2=(\sqrt{s_{11}s_{22}})_2. \quad (A9j)$$

It is interesting to note that the effect of β in the overall solution is introduced only through the coefficients Qs and Q^*s. Since for most practical bi-material combinations the value of β is usually small, it is proposed to take $\beta = 0$. This simplifies the expressions for Qs considerably. For $\beta = 0$, the expressions for Qs and Q^*s reduces to

$$Q_1=\frac{[2\Sigma]}{\left[\Sigma+\left(\frac{n_1}{n_2}\right)\Lambda\right]} \quad (A10a)$$

$$Q_2=Q_3=0 \quad (A10b)$$

$$Q_4=\frac{[2\Sigma\Lambda]}{\left[\Lambda\Sigma+\left(\frac{n_1}{n_2}\right)\right]} \quad (A10c)$$

$$Q_1^*=\frac{\left[1-\left(\frac{n_1}{n_2}\right)\left(\frac{\Lambda}{\Sigma}\right)\right]}{\left[1+\left(\frac{n_1}{n_2}\right)\left(\frac{\Lambda}{\Sigma}\right)\right]} \quad (A10d)$$

$$Q_2^*=Q_3^*=0 \quad (A10e)$$

$$Q_4^*=\frac{\left[1-\left(\frac{n_1}{n_2}\right)\left(\frac{1}{\Sigma\Lambda}\right)\right]}{\left[1+\left(\frac{n_1}{n_2}\right)\left(\frac{1}{\Sigma\Lambda}\right)\right]} \quad (A10f)$$